Available online at http://www.journalcra.com

International Journal of Current Research
Vol. 6, Issue, 01, pp.4532-4538, January, 2014

INTERNATIONAL JOURNAL OF CURRENT RESEARCH

ISSN: 0975-833X

RESEARCH ARTICLE

GREEN, EFFECTIVE BIOLOGICAL ROUTE FOR THE SYNTHESIS OF SILVER NANOPARTICLES USING CYPERUS ROTUNDUS GRASS EXTRACTS

[1]Siva, S., [2]Sulaiman Sameem, M., [3]Sudharsan S. and [*,1]Sayee Kannan, R.

[1]PG Research and Department of Chemistry, Thiagarajar College, Madurai-625 009, India
[2]Block Research Teacher Educator, SSA, Madurai-625008
[3]Department of Chemistry, PSR Engg College, Sivakasi- 626 140, India

ARTICLE INFO

Article History:
Received 15th September, 2013
Received in revised form
26th October, 2013
Accepted 09th December, 2013
Published online 26th January, 2014

Key words:
Cyperus rotundus,
Silver nanoparticles,
Biological reduction,
Green synthesis.

ABSTRACT

Development of consistent and eco-friendly processes for the synthesis of metallic nanoparticles is an essential requisite nowadays. Herein we present the distinct properties of the silver nanoparticles (AgNPs) synthesized using hot water Cyperus Rotundus Grass Extracts (CRGE) a reducing and capping agent. The nature of AgNPs synthesized was analyzed by Atomic Force Microscope (AFM), Scanning Electron Microscope (SEM), energy-dispersive microanalysis (EDX), X-ray diffraction spectroscopy (XRD), Flourier Transform Infra Red (FTIR), Thermo Gravimetric Analysis (TGA), Differential Thermal Analysis (DTA) and UV–vis spectroscopy (UV). UV spectral analysis showed silver surface Plasmon resonance band at 425nm. XRD showed that the particles were crystalline in nature with face centered cubic structure of the bulk silver with broad peaks at 35.62°, 38.24 °, 46.42 °, 55.00 °, 64.5 °, 78 °. Morphologically, the nanoparticles were found to be spherical with an average particle size distribution of 1 to 100 nm. CRGE demonstrated strong potential for synthesis of silver nanoparticles by rapid reduction of silver ions (Ag^+ to Ag^o).

INTRODUCTION

Nanoparticles, the fundamental blocks of nanotechnology exhibit larger surface area to volume ratio. Today, the most effectively studied nanoparticles are made from noble metals *viz.,* Ag, Pt, Pd and Au. Among those, silver nanoparticles play an eminent role in the versatile applications of Chemistry and biology. It has been also successively used in sanitizing air, water and hazardous wastes. Silver nanoparticles have been synthesized using various plant extracts such as Hibiscus rosa sinensis (Philip, 2010), Svensonia hyderabadensis (Rao and Savithramma, 2011), Trianthema decandra (Geethalakshmi and Sarada, 2010), Dioscorea batatas (Nagajyothi and Lee, 2011), Moringa oleifera (Prasad and Elumalai, 2011), Bacopa monniera (Mahitha *et al*., 2011), Citrus limon (Prathna *et al*., 2011), Arbutus unedo (Kouvaris *et al*, 2012), Acalypha indica (Krishnaraj *et al*., 2010), Mentha piperita (Ali *et al*., 2011), Cassia auriculata (Udayasoorian *et al*., 2011) etc. So far, the AgNPs has not been synthesized using CRGE. Hence, we report an inexpensive and reproducible method for the large-scale synthesis of silver nanoparticles using CRGE. Here CRGE acts as reducing, encapsulating and stabilizing agent. In this study, we explored the potential of the Cyperus rotundus (C. rotundus) to enlarge the scope of non-toxic biological systems for the biosynthesis of AgNPs.

Corresponding author: Sayee Kannan, R.
PG Research and Department of chemistry, Thiagarajar College, Madurai-625 009, India.

MATERIALS AND METHODS

Materials

The raw plant material used in the present study was C. rotundus. This is a plant material freely available in Tamil Nadu, India (Fig.1). AR grade SD fine silver nitrate ($AgNO_3$) was purchased and its 0.1 M solution was prepared in stock and diluted to 1 mM solution. The other chemicals and reagents were of chemically pure grade (AnalaR) procured from SD Fine Chemicals, India.

Methods

Preparation of CRGE

Fresh C. rotundus grass were collected and washed with sterile distilled water and dried. After drying cut in to small pieces. The extract was prepared by taking 20 g of thoroughly washed finely cut C. rotundus grass in a 250-mL Erlenmeyer flask with 100 mL of deionized water, and then boiling the mixture at 60 °C for 5 min. After boiling, the solution was decanted and filtered through nylon mesh (spectrum). The filtrate is used as reducing agent and stabilizer, stored at 4ºC for further nanoparticles synthesis process.

Green synthesis of AgNPs

For synthesis process, the 2 mL of CRGE was added to 25 mL of 1 mM $AgNO_3$ aqueous solution and the resulting solution

became brown in color. Then the mixture was stirred for 30 min to obtain the AgNPs. Here the formation of AgNPs was identified by change in the color of the stock solution to brown within 20 min (Fig.2). These biologically-reduced aqueous solutions of Ag nanoparticles were used for further characterizations. This process carried out at room temperature.

Fig.1. Photography of Cyperus rotundus grass

Fig.2 (a) Silver nitrate mixture before (b) grass extracts and (c) After the synthesis of AgNPs

Spectral analysis

The synthesized AgNPs were confirmed by sampling the aqueous component of different time intervals and the absorption maxima was scanned by UV-Vis spectrophotometer at the wavelength of 300-800 nm on UV-1800 SHIMADZU spectrophotometer. The infrared spectra were achieved in a Shimadzu FT-IR spectrophotometer IR Affinity-1 by employing KBr pellets and registering amplitude waves ranging from 400 to 4000 cm^{-1}.

Morphological analysis

Morphological analysis was done using Philips model CM 200 SEM machine. Thin films of the sample were prepared on a carbon coated copper grid by just dropping a very small amount of the grid, extra solution was removed using a blotting paper and then the films on the SEM grid were allowed to dry by putting it under mercury lamp for 5 min.

Structural analysis

The formation and quality of compounds were checked using X'Pert Pro Materials Research diffractometer system. The XRD pattern was measured by drop coated films of $AgNO_3$ on glass plate and employed with characteristic radiation in the range of 20^0 to 90^0 at a scan rate of 0.05^0/min with the time constant of 2 s, CuK_α radiation and amplitude wave $\lambda = 1.5418$ Å working with a 40 kV voltage and 30 mA current. The full–width at half–maximum (FWHM) from three different peaks were used in Scherrer's equation to determine the average crystallite size of the nanoparticles.

AFM analysis

A small volume of sample was spread on a well cleaned glass cover slip surface mounted on the AFM stub, and dried with nitrogen flow at room temperature. Images were obtained in tapping mode using a silicon probe cantilever and resonance frequency 209-286 KHz, spring constant. The scan rate used was 1 HKz. A minimum of five images for each sample were obtained with AFM and analyzed to ensure reproducible results.

RESULTS AND DISCUSSION

Spectral characterization

UV–Vis spectra

The colour change in reaction mixture (metal ion solution + grass extract) was recorded through visual observation. The color change showed the presence of silver nanoparticles in the grass extract and it was characterized by UV-Visible spectrophotometer. The strong surface plasmon resonance band positioned at 425 nm was observed for AgNPs (Fig.3). The position of SPR band in UV–Vis spectra is sensitive to particle shape, size, its interaction with the medium, local refractive index and the extent of charge transfer between medium and the particles. The broad spectra indicate the presence of particles with a broad size distribution (Sosa *et al*, 2003).

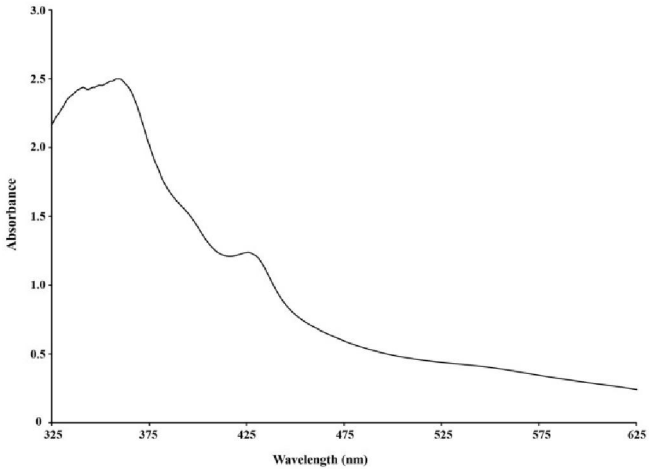

Fig.3. UV-Visible Spectra of the synthesized AgNPs

FT-IR spectra

FT-IR spectroscopy is used to probe the chemical composition of the surface of the AgNPs and the local molecular environment of the capping agents on the nanoparticles. The FT-IR spectrum of CRGE mediated AgNPs is shown in Fig. 4. The band at 3428 cm^{-1} corresponds to intermolecular O-H stretching vibrations. The peaks at 2854 and 2924 cm^{-1} are belonging to C-H aromatic stretching frequencies. The medium absorption peak located at 1699 & 1743 cm^{-1} is identified as the amide group. This amide band occurs due to carbonyl stretch and N–H deformation vibrations in the amide linkage of proteins present in it. The band observed at 1456 cm^{-1} may be due to the C–O–H vibrations. The band at 1267 cm^{-1} is assigned to polyphenols. The band at 2362 cm^{-1} corresponds to C–N stretching vibrations of aliphatic amines (Suman *et al*., 2013). All these bands clearly confine the presence of polyphenols, proteins, tannins and flavonoids in CRGE which act as reducing agents for the synthesis of silver nanoparticles. Thus, the IR spectroscopic study confirmed that the CRGE has the ability to perform dual functions of reduction and stabilization of AgNPs.

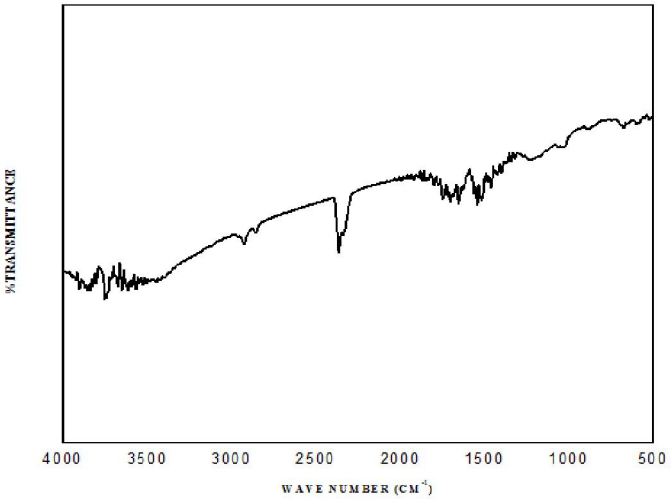

Fig.4. IR Spectra of the synthesized AgNPs

SEM

The synthesized nanoparticle morphology was characterized by SEM was done by using Philips model CM 200 instrument. After the completion of reaction, the nanoparticles placed on carbon coated copper grid, it exhibit spherical in shape (Fig.5). Further, from all the SEM images it is evident that the morphology of silver nanoparticles is nearly spherical which is in good agreement with the shape of SPR band in the UV–Vis spectra. The size of the AgNPs range around 1 -100nm (Sankar *et al*., 2013).

EDAX

CRGE reduced silver solutions were dried, drop coated on to glass film. The EDAX pattern thus clearly shows that the silver nanoparticles are crystalline in nature by the reduction of silver ions by using grass broth. It expose strong signal in the silver region and confirms the formation of AgNPs (Fig.6). Metallic silver nano crystals generally show typical optical absorption peak approximately at 3 keV due to surface plasmon resonance (kannan *et al*., 2011). Other elemental signals are recorded possibly due to elements from enzymes or proteins present within the grass extract.

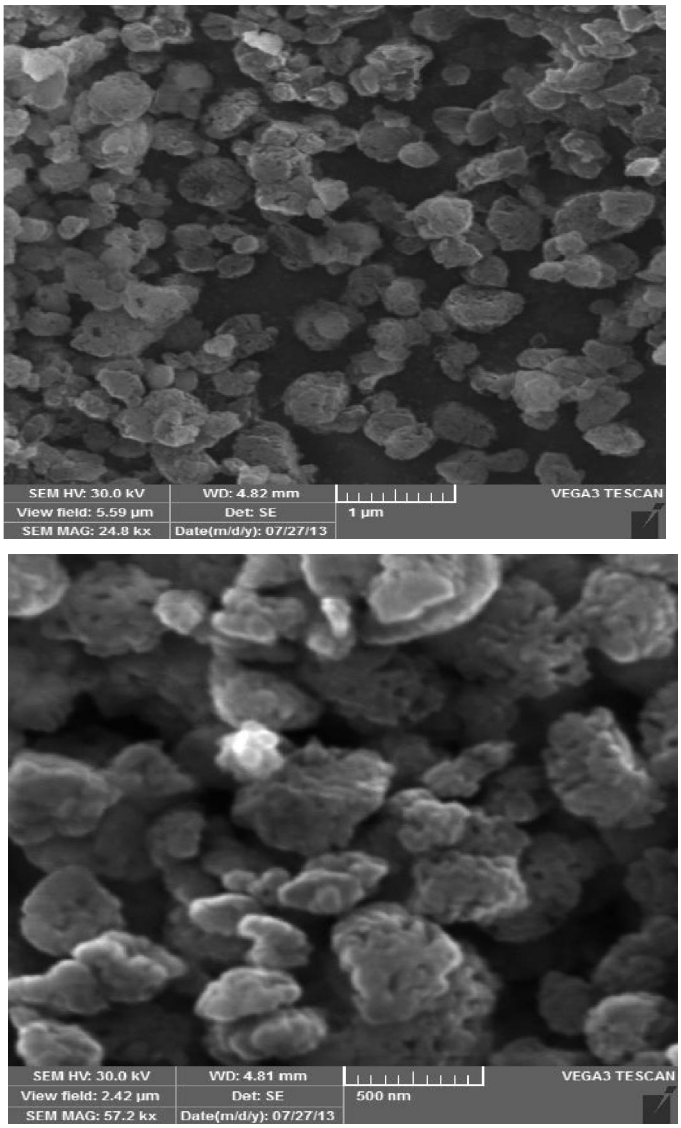

Fig.5. SEM image of AgNPs using CRGE leaf extract

XRD

The XRD pattern of the AgNPs is as shown in Fig. 7 and Table 1. The prominent diffraction peaks observed are indexed to (1 0 0), (1 0 1), (1 0 3), (0 0 6), (1 1 0) and (2 0 2) reflections of face centered cubic structure of metallic silver, respectively revealing that the synthesized AgNPs are composed of pure crystalline silver (JCPDS file no. 87-0598). The relative intensity of the (1 0 0) plane to (2 0 2) diffraction peaks in the figure was higher than the conventional value. This indicates that the prepared AgNPs may be enriched in (1 1 1) facets and thus the (1 1 1) plane seems to be preferentially oriented parallel to the surface of the supporting substrate (Gurusamy and Cellapandian, 2013). The average particle size of AgNPs can be calculated using Debye–Scherrer equation: $D = k\lambda/\beta\cos\theta$, where D is the thickness of the nanocrystal, k is a constant, λ is the wavelength of X–rays and β is the full width at half maxima of (111) reflection at Bragg's angle 2θ. The average particle size calculated from the XRD patterns is 24.26 nm and it is in good agreement with the particle size assigned from the SEM studies.

Table 1. XRD PROFILE OF AgNPs

Peak Pos. [°2Th.]	FWHM Left [°2Th.]	d-spacing, [Å]	hkl values	Crystallite size [nm]
35.62	0.052	2.51828	1 0 0	45.52
38.24	0.4	2.35156	1 0 1	7.037
46.42	0.22	1.95468	1 0 3	12.12
55.00	0.12	1.66829	0 0 6	22.79
64.5	0.06	1.44257	1 1 0	52.56
78	1	1.22991	2 0 2	5.56
Average crystallite size (nm)				24.26

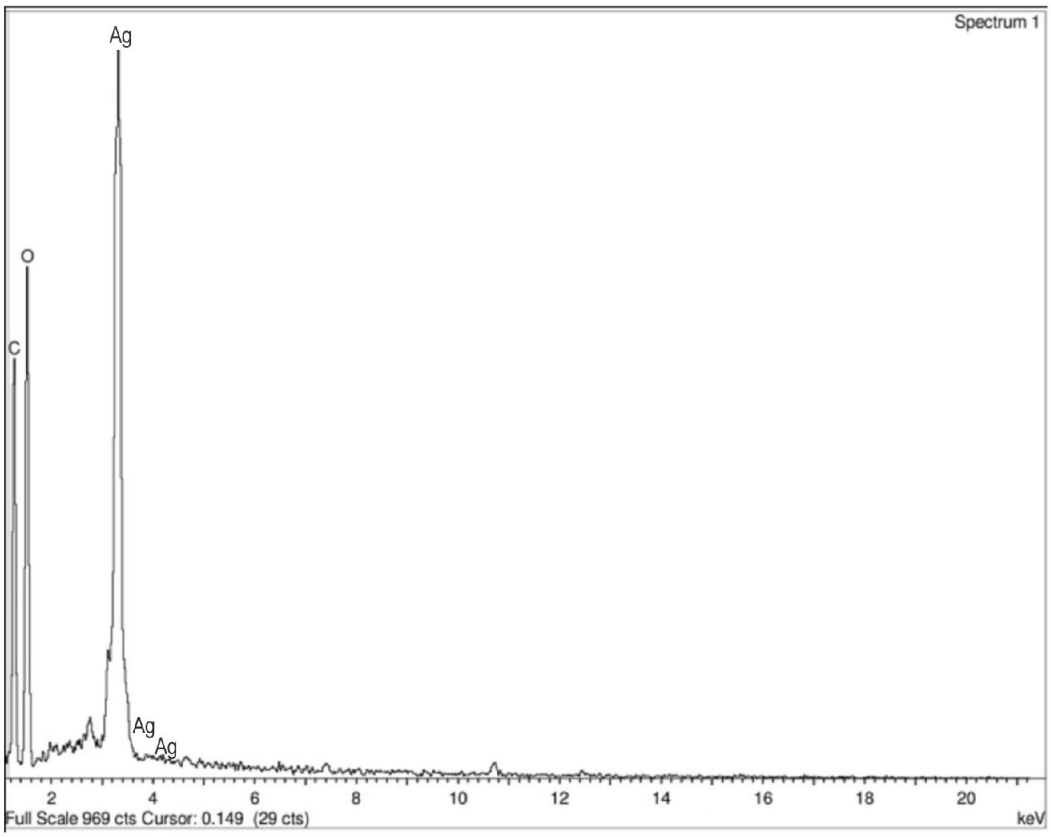

Fig.6. EDX spectra of AgNPs

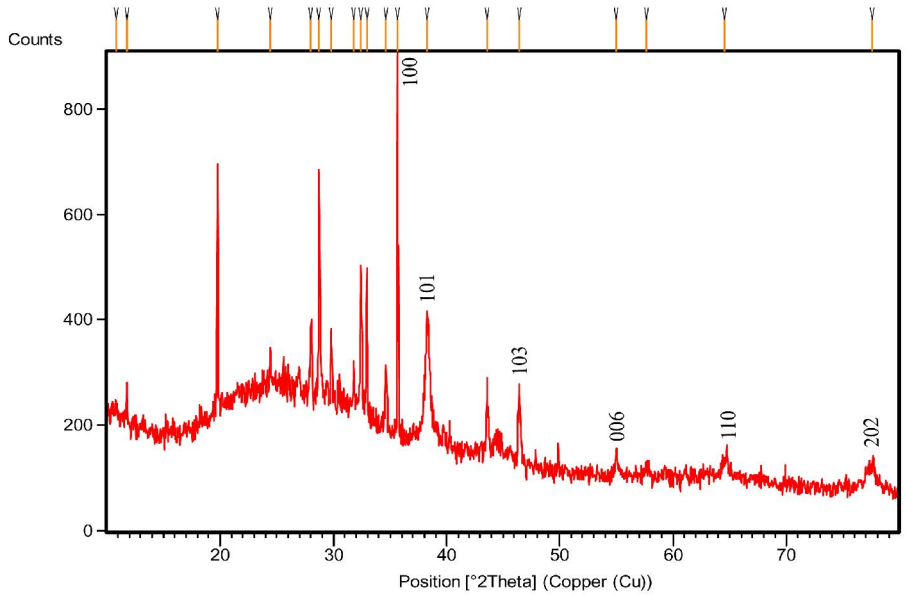

Fig. 7. X-ray diffraction pattern of AgNPs

AFM

AFM analysis predominantly assures the homogeneity and the respective size of the synthesized particles. Here, the AgNPs reduced by CRGE were characterized by AFM for confirming its detail size, morphology and agglomeration of the particles. From all the figures (Figs. 8, 9 and 10), it has been notified that the biologically reduced nanoparticles are in the range of 10 nm. Further, the clear particle shape of the nanoparticles is also observed from their surface topography (Fig. 8). The size distribution of the synthesized AgNPs is showed in the histogram, which ranges from 1 to 5 nm. The nanoparticles are maximum at 5nm is also showed in the line profile. The statistics graph is also showed that the size distribution of nanoparticles, this ranges from around 1 to 11 nm. In addition, the uniform spherical nature of our synthesized nanoparticles is also confirmed from the inset image observed from AFM (Fig. 9). Thus, from the AFM observations, it is clearly confined that the synthesized nanoparticles are formed without agglomeration and are spherical in nature (Fig. 10). All the results achieved here are in good agreement with the spectral and XRD pattern analysis (Raman *et al*., 2012).

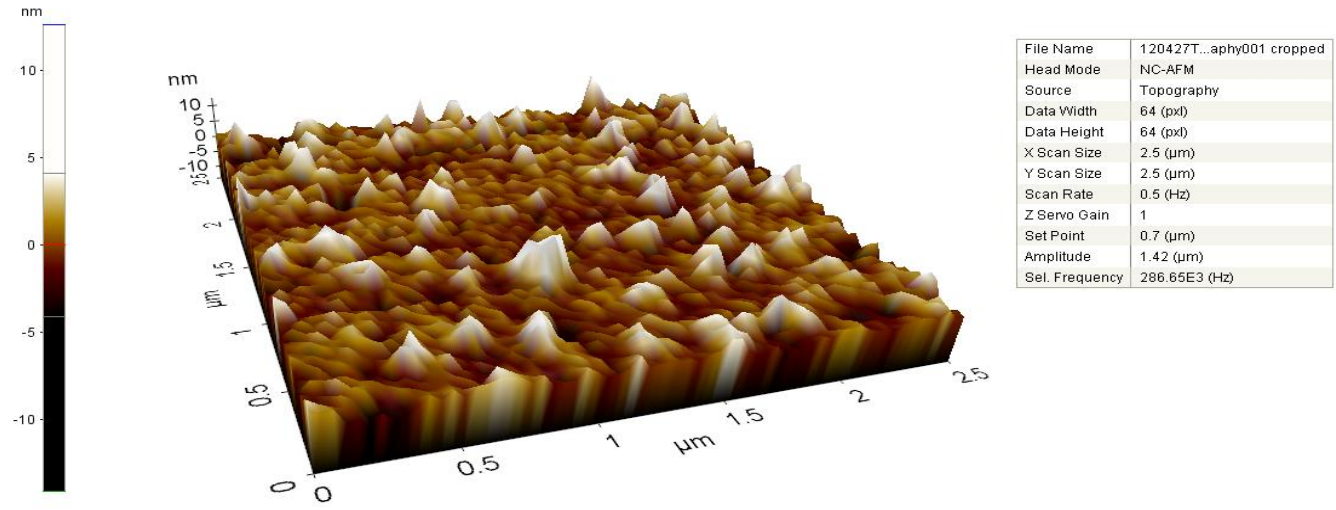

Fig. 8. AFM topographical image of AgNPs

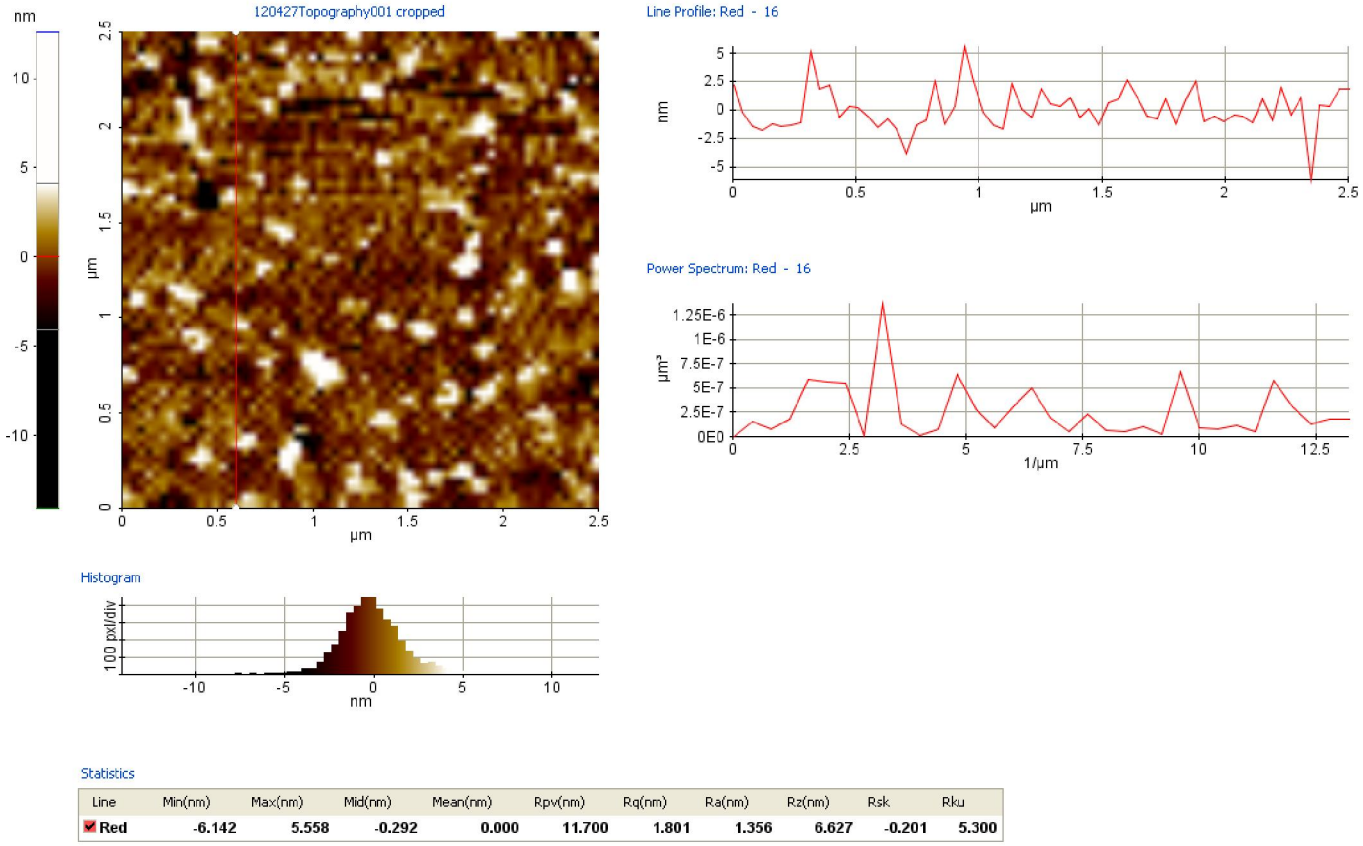

Fig. 9. AFM size distribution image of AgNPs

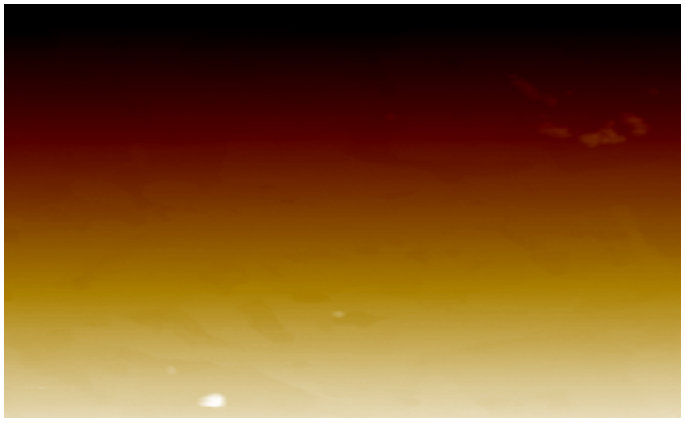

Fig. 10. AFM inset image of AgNPs

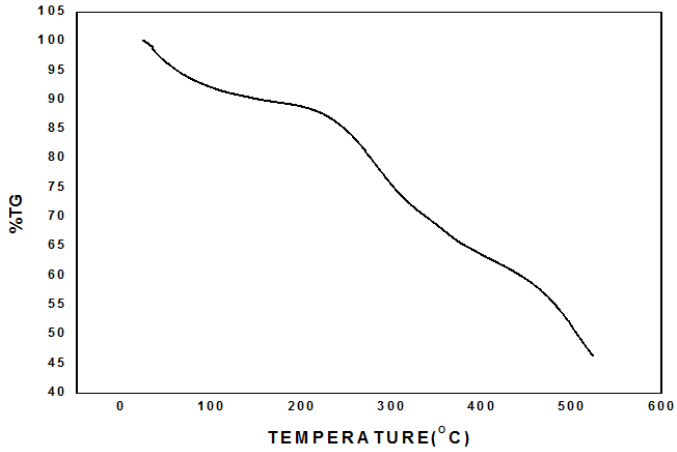

Fig. 11. TG curve of the AgNPs at different temperatures

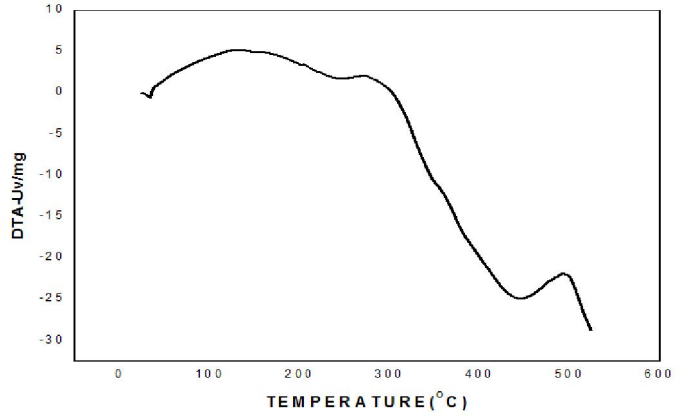

Fig. 12. DTA curve of the AgNPs at different temperatures

TGA

The weight loss of AgNPs during the heating process was investigated Fig. 11. The TG curve of AgNPs revealed weight loss at two regions corresponding to the loss of water (8% by weight) at temperature around 100°C and the loss of organic binder (50% by weight) at the temperature range of 200–500°C. Such total weight loss at 30–500°C of TG curve related to the total weight of organic binder added. No further significant weight loss peak was observed in the temperature range above 500°c. It can be concluded that AgNPs exhibited thermal stability during the heating process at the temperature range 500°C.

DTA

Fig. 12 shows the loss of water and organic binder of AgNPs was evidenced by One endothermic and exothermic peak around 100 and 480°C corresponding to the evaporation of water and the oxidation of organic binder. From DTA curve, it is concluded that the limiting temperature for the safer use of AgNPs was 100°C since the AgNPs degrade thermally after 100°C (Thongnopkun *et al*., 2012).

Conclusion

In this present work, we have built-up a simple and green method to synthesize AgNPs with diameters in the range of 1–100nm using the CRGE as reductant and capping agent. The grass extract has a syndicate effect in reducing the silver salt solution and hindering the particle growth. This green chemistry approach also serves in scaling up and economic viability of the synthetic process. Further, it is also notable that the reduction of silver ions and stabilization of AgNPs may occur through the involvement of tannins and flavonoids present in CRGE. This biosynthesis may also favors lower toxicity to environment denoting its merit and prompt for preference in various industrial and medical applications.

Acknowledgement

The authors thank the Principal and Management of Thiagarajar College for providing facilities and encouragement. The authors also thank the Department of Chemistry, A.N.J.A.C, Sivakasi and V.H.N.S.N.C, V.N.R. Referee for the valuable comments.

REFERENCES

Ali, D.M., Thajuddin, N., Jeganathan, K., and Gunasekaran, M., 2011. Plant extract mediated synthesis of silver and gold nanoparticles and its antibacterial activity against clinically isolated pathogens. Colloids Surf B. 85, 360–365.

Geethalakshmi, R., and Sarada, D.V.L., 2010. Synthesis of plant-mediated silver nanoparticles using Trianthema decandra extract and evaluation of their anti microbial activities. IJIRSET. 2, 970-975.

Gurusamy, A., and Cellapandian, K., 2013. Green Synthesis of Silver Nanoparticles using Millingtonia hortensis and Evaluation of their Antimicrobial Efficacy. *Inter.J.Nanomater.Bios*. 3 (1), 21-25.

Kannan, N., Mukunthan, K.S., and Balaji, S., 2011. A comparative study of morphology, reactivity and stability of synthesized silver nanoparticles using Bacillus subtilis and Catharanthus roseus (L.) G. Don. Colloids Surf B. 86, 378–383.

Kouvaris, P., Delimitis, A., Zaspalis, V., Papadopoulos, D., Tsipas, S.A., and Michailidis, N., 2012. Green synthesis and characterization of silver nanoparticles produced using Arbutus unedo leaf extract. Materials Lett. 76, 18-20.

Krishnaraj, C., Jagan, E.G., Rajasekar, S., Selvakumar, P., Kalaichelvan, P.T., and Mohan, N., 2010. Synthesis of

silver nanoparticles using Acalypha indica leaf extracts and its antibacterial activity against water borne pathogens. Colloids Surf B. 76, 50-56.

Mahitha, B., Deva, B., Raju, P., Dillip, G.R., Reddy, C.M., Mallikaruna, K., Manoj, I., Priyanka, S., Rao, K.J and Sushma, N.J., 2011. Biosynthesis, Charecterization and antimicrobial studies of AgNPs extract from Bacopa monniera whole plant. *Dig J Nanomater Biostruct*. 6, 135-142.

Nagajyothi, P.C., and Lee, K.D., 2011. Synthesis of Plant-Mediated Silver Nanoparticles Using Dioscorea batatas Rhizome Extract and Evaluation of their Antimicrobial Activities. *J.Nano Mat.* 10, 1155-2011.

Philip, D., 2010. Green synthesis of gold and silver nanoparticles using Hibiscus Rosa sinensis. Physica E. 42, 1417–1424.

Prasad, T.N.V.K.V., and Elumalai, E.K., 2011. Biofabrication of Ag nanoparticles using Moringa oleifera leaf extract and their antimicrobial activity. *Asian Pac J Trop Biomed*.1 (6), 439-443.

Prathna, T.C., Chandrasekaran, N., Raichur, A. M., and Mukherjee, A., 2011. Biomimetic synthesis of silver nanoparticles by Citrus limon (lemon) aqueous extract and theoretical prediction of particle size. Colloids Surf. 82, 152–159.

Raman, N., Sudharsan, S., Veerakumar, V., Pravin, N., and Vithiya, K., 2012. Pithecellobium dulce mediated extra-cellular green synthesis of larvicidal silver nanoparticles. Spectrochim. Acta A.Mol. Biomo. Spectrosc. 96, 1031–1037.

Rao, M.L., and Savithramma, N., 2011. Biological Synthesis of Silver Nanoparticles using Svensonia Hyderabadensis Leaf Extract and Evaluation of their Antimicrobial Efficacy. *J. Pharm. Sci. & Res.* 3, 1117-1121.

Sankar, R., Karthik, A., Prabu, A., Karthik, S., Subramanian, K., and Ravikumar, V., 2013. Origanum vulgare mediated biosynthesis of silver nanoparticles for its antibacterial and anticancer activity. Colloids Surf B. 108, 80– 84.

Sosa, I.O., Noguez, C., and Barrera, R.G., 2003. Optical properties of metal nanoparticles with arbitrary shapes. *J. Phys. Chem.* 107, 6269–6275.

Suman, T.Y., Radhika Rajasree, S.R., Kanchana, A and Beena, S., 2013. Elizabeth Biosynthesis, characterization and cytotoxic effect of plant mediated silver nanoparticles using Morinda citrifolia root extract. Colloids Surf B. 106, 74– 78.

Thongnopkun, P., Jamkratoke, M., and Ekgasit, S., 2012. Thermal behavior of nano silver clay in the application of handmade jewelry. Mater. Sci. Eng. 556, 849–854.

Udayasoorian, C., Kumar, R.V., Jayabalakrishnan, M., 2011. Extracellular synthesis of silver nanoparticles using leaf extract of Cassia auriculata. *Dig J Nanomater Biostruct*. 6 (1), 537-543.

****